



Public Health
England



NHS Breast Screening Programme Equipment Report

Technical evaluation of Siemens Revelation
digital breast tomosynthesis system

March 2019

Available from the National Co-ordinating Centre
for the Physics of Mammography (NCCPM)

About Public Health England

Public Health England exists to protect and improve the nation's health and wellbeing, and reduce health inequalities. We do this through world-leading science, knowledge and intelligence, advocacy, partnerships and the delivery of specialist public health services. We are an executive agency of the Department of Health and Social Care, and a distinct delivery organisation with operational autonomy. We provide government, local government, the NHS, Parliament, industry and the public with evidence-based professional, scientific and delivery expertise and support.

Public Health England, Wellington House, 133-155 Waterloo Road, London SE1 8UG
Tel: 020 7654 8000 www.gov.uk/phe
Twitter: [@PHE_uk](https://twitter.com/PHE_uk) Facebook: www.facebook.com/PublicHealthEngland

About PHE Screening

Screening identifies apparently healthy people who may be at increased risk of a disease or condition, enabling earlier treatment or informed decisions. National population screening programmes are implemented in the NHS on the advice of the UK National Screening Committee (UK NSC), which makes independent, evidence-based recommendations to ministers in the 4 UK countries. PHE advises the government and the NHS so England has safe, high quality screening programmes that reflect the best available evidence and the UK NSC recommendations. PHE also develops standards and provides specific services that help the local NHS implement and run screening services consistently across the country.

www.gov.uk/phe/screening Twitter: [@PHE_Screening](https://twitter.com/PHE_Screening) Blog: phescreening.blog.gov.uk

Prepared by: N Tyler, A Mackenzie, KC Young

For queries relating to this document, please contact: phe.screeninghelpdesk@nhs.net

The image on page 7 is courtesy of Siemens.

OGL

© Crown copyright 2019

You may re-use this information (excluding logos) free of charge in any format or medium, under the terms of the Open Government Licence v3.0. To view this licence, visit [OGL](https://www.ogil.io). Where we have identified any third party copyright information you will need to obtain permission from the copyright holders concerned.

Published March 2019

PHE publications

gateway number: GW-251

PHE supports the UN

Sustainable Development Goals



SUSTAINABLE DEVELOPMENT GOALS

Contents

About Public Health England	2
About PHE Screening	2
Contents	8
Executive summary	4
1. Introduction	5
1.1 Testing procedures and performance standards for digital mammography	5
1.2 Objectives	5
2. Methods	6
2.1 System tested	6
2.2 Dose and contrast-to-noise ratio using AEC	8
2.3 Image quality measurements	9
2.4 Geometric distortion and reconstruction artefacts	9
2.5 Alignment	11
2.6 Image uniformity and repeatability	11
2.7 Detector response	11
2.8 Timings	11
2.10 Local dense area	12
3. Results	14
3.1 Dose and contrast-to-noise ratio using AEC	14
3.2 Image quality measurements	16
3.3 Geometric distortion and resolution between focal planes	17
3.4 Alignment	19
3.5 Image uniformity and repeatability	19
3.6 Detector response	20
3.7 Timings	20
3.8 Modulation Transfer Function	21
3.9 Local dense area	22
4. Discussion	24
4.1 Dose and contrast-to-noise ratio	24
4.2 Image quality	24
4.3 Geometric distortion and reconstruction artefacts	24
4.4 Alignment	25
4.5 Image uniformity and repeatability	25
4.6 Modulation transfer function	25
4.7 Local dense area	25
5. Conclusions	26
References	27

Executive summary

The technical performance of the Siemens Revelation digital breast tomosynthesis system was tested in tomosynthesis mode. The evaluation of the performance in 2D mode is published as a separate report. The mean glandular dose (MGD) to the standard breast was found to be 1.34mGy, which is below the dose limiting value of 2.5mGy for tomosynthesis in the EUREF protocol.

Technical performance of this equipment was found to be satisfactory, so that the system could proceed to practical evaluation in a screening centre. This report provides baseline measurements of the equipment performance including:

- dose
- contrast detail detection
- contrast-to-noise ratio (CNR)
- reconstruction artefacts, z-resolution
- detector response
- projection modulation transfer function (MTF)

Available from the National Co-ordinating Centre
for the Physics of Mammography (NCCPM)

1. Introduction

1.1 Testing procedures and performance standards for digital mammography

This report is one of a series evaluating commercially available digital breast tomosynthesis systems on behalf of the NHS Breast Screening Programme (NHSBSP).¹⁻⁵ The testing methods and standards applied are those of the relevant NHSBSP protocols, which are published as NHSBSP Equipment Reports. Report 1407⁶ describes the testing of digital breast tomosynthesis systems.

The NHSBSP protocol is similar to the EUREF protocol⁷, but the latter also provides additional or more detailed tests and standards, some of which are included in this evaluation.

1.2 Objectives

The aim of the evaluation was to measure the technical performance of the Siemens Revelation system in tomosynthesis mode.

Available from the National Co-ordinating Centre
for the Physics of Mammography (NCCPM)

2. Methods

2.1 System tested

The tests were conducted at the Siemens factory in Forchheim, Germany, on the Revelation system. Details of the system tested are given in Table 1.

Table 1. System description

Manufacturer	Siemens
Model	Revelation
System serial number	114
Target material	Tungsten (W)
Added filtration	50 μ m Rhodium (Rh)
Detector type	Amorphous Selenium
Detector serial number	LV2-00007
Image pixel size	85 μ m
Detector size	239mm x 305mm
Pixel array	2816 x 3584
Source to table distance	638mm
Source to detector distance	655mm
Automatic exposure control (AEC) mode	OPDOSE, segmentation on or off, 5 dose levels: normal \pm 10 or 20%.
Tomosynthesis projections	25 projections covering range \pm 25°
Centre of rotation	30 mm above breast support
Anti-scatter grid	Grid not used
Reconstructed focal planes	Focal planes at 1mm intervals
Software version	VC10B

In both 2D and tomosynthesis modes OPDOSE is used for automatic exposure control (AEC) and is based on compressed breast thickness. The system acquires a preliminary stationary 2D image (tube load 5mAs) at a tube angle of 0 degrees, the tube then moves into position for the first projection which commences at approximately -25 degrees. The tube load for tomosynthesis is calculated using the preliminary zero degree exposure and divided equally between the subsequent 25 projections.

The maximum compressed breast thickness (CBT) that can be reconstructed in tomosynthesis mode is 100mm. For thicknesses above this, the system will allow the exposure but will display a warning that only the lower 100mm will be reconstructed.

There is a mode to automatically perform combination exposures, comprising a 2D and a tomosynthesis exposure in the same compression.

Table 2. Image file sizes for 60mm CBT, 24cm x 30cm field size

Format	Pixels per frame	Frames per image	Total image file size (MB)
Projections	2816x3584	26	507
Planes	2816x3584	61	821

Examples of the image file sizes are shown in Table 2. The projection images comprise of 25 images for the reconstruction and one image used for setting the exposure level. The file size of the reconstructed volume depends on the CBT and field size.

The Revelation is shown in Figure 1.

Figure 1. The Siemens Revelation digital breast tomosynthesis system



2.2 Dose and contrast-to-noise ratio using AEC

2.2.1 Dose measurement

To calculate the MGD to the standard breast, measurements were made of the half value layer (HVL) and tube output, at the available kV and target/filter combinations. The output measurements were made on the midline at the standard position of 40mm from the chest wall edge (CWE) of the breast support platform. The compression paddle was in the beam, raised well above the ion chamber.

In tomosynthesis mode, exposures of a range of thicknesses of polymethyl methacrylate (PMMA) were made using AEC. For each measurement the height of the paddle was set to the equivalent breast thickness for that thickness of PMMA. Spacers were positioned at the nipple edge of the field, so as not to affect the operation of the AEC.

The method of measuring tomosynthesis doses described in the UK protocol differs slightly from the method described by Dance et al.⁸ The incident air kerma is measured with the compression paddle well above, instead of in contact with, the ion chamber. Measurements on other systems^{1,2} show that this variation reduces the air kerma and thus the mean glandular dose (MGD) measurement by 3% to 5%. Otherwise the MGDs in tomosynthesis mode were calculated using the method described by Dance et al.⁸ This is an extension of the established 2D method, using the equation:

$$D = KgcsT \quad (1)$$

where D is the MGD (mGy), K is the incident air kerma (mGy) at the top surface of the PMMA blocks, and g , c and s are conversion factors. The additional factor, T , is derived by summing weighted correction factors for each of the tomosynthesis projections. Values of T are tabulated⁷ for the Siemens Inspiration for different CBTs, and the same values are appropriate for the Revelation, because it has the same geometry.

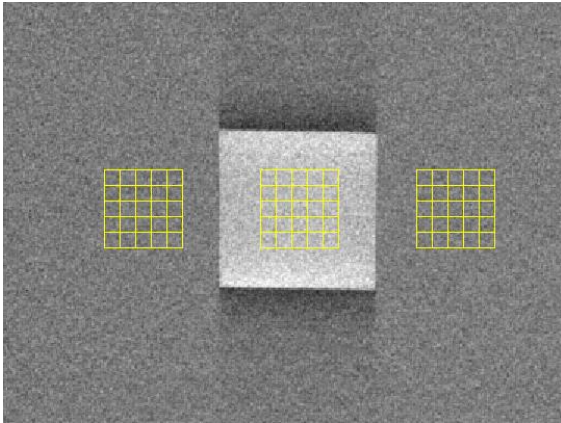
2.2.2 Contrast-to-noise ratio

For contrast-to-noise ratio (CNR) measurements, a 10mm x 10mm square of 0.2mm thick aluminium foil was included in the PMMA phantom, positioned 10mm above the table on the midline, 60mm from the CWE.

The CNR was measured in the focal plane in which the aluminium square was brought into focus. The 5mm x 5mm regions of interests (ROI) were subdivided into 1mm x 1mm elements and the background ROIs were positioned adjacent to the aluminium square, as shown in Figure 2. The mean pixel values and their standard deviations were averaged over all the 1mm x 1mm elements, and the CNR was calculated from these averages.

CNR was also assessed in the unprocessed tomosynthesis projections acquired for these images. The variation in central projection CNR with PMMA thickness and the variation in projection CNR with projection angle for a 45mm thick PMMA block were also assessed.

Figure 2. The position of 5mm x 5mm ROIs for assessment of CNR. (The CWE is to the left)



2.3 Image quality measurements

A CDMAM phantom (Version 3.4, serial number 1022, UMC St. Radboud, Nijmegen University, Netherlands) was positioned between 2 blocks of PMMA, each 20mm thick. The breast support is sloped and so a spacer of 5mm was used at the front of the blocks to ensure the plane of the CDMAM phantom was parallel to the detector. The exposure factors were chosen to be close to those selected by the AEC, when imaging a 50mm thick block of PMMA. This procedure was repeated to obtain a representative sample of 16 images at this dose level. Two further sets of 16 images at double and half of this dose were then acquired.

The focal plane corresponding to the vertical position of the CDMAM phantom within the image was extracted from each reconstructed stack of images. The sets of CDMAM images were read and analysed using 2 software tools: CDCOM version 1.6 (www.euref.org) and CDMAM Analysis version 2.1 (NCCPM, Guildford, UK). This was repeated for 2 focal planes immediately above and below the expected plane of best focus to ensure that the threshold gold thickness quoted corresponded to the best image quality obtained.

2.4 Geometric distortion and reconstruction artefacts

The relationship between reconstructed tomosynthesis focal planes and the physical geometry of the volume that they represent was assessed. This was done by imaging a geometric test phantom consisting of a rectangular array of 1mm diameter aluminium balls at 50mm intervals in the middle of a 5mm thick sheet of PMMA. The phantom was placed at various heights (7.5, 32.5, and 52.5mm) within a 60mm stack of plain sheets of PMMA. The block of PMMA was tilted using the same method as used in section 2.3. Reconstructed tomosynthesis planes

were analysed to find the height of the focal plane in which each ball was best in focus, the position of the centre of the ball within that plane, and the number of adjacent planes in which the ball was also seen. The variation in appearance of the ball between focal planes was quantified.

This analysis was automated using a software tool developed at the National Coordinating Centre for the Physics of Mammography (NCCPM) for this purpose. This software is in the form of a plug-in for use in conjunction with ImageJ (<http://rsb.info.nih.gov/ij/>).

2.4.1 Height of best focus

For each ball, the height of the focal plane in which it was best in focus was identified. Results were compared for all balls within each image, to judge whether there was any tilt of the test phantom relative to the reconstructed planes, or any vertical distortion of the focal planes within the image.

2.4.2 Positional accuracy within focal plane

The x and y co-ordinates within the image were found for each ball (x and y are perpendicular and parallel to the CWE, respectively). The mean distances between adjacent balls were calculated, using the pixel spacing quoted in the DICOM image header. This was compared to the physical separation of balls within the phantom, to assess the scaling accuracy in the x and y directions. The maximum deviations from the mean x and y separations were calculated, to indicate whether there was any discernible distortion of the image within the focal plane.

2.4.3 Appearance of the ball in adjacent focal planes

Changes to the appearance of a ball between focal planes were assessed visually.

To quantify the extent of reconstruction artefacts in focal planes adjacent to those containing the image of the balls, the reconstructed image was treated as though it were a true 3-dimensional volume. The software tool was used to find the z-dimension of a cuboid around each ball which would enclose all pixels with values exceeding 50% of the maximum pixel value. The method used was to re-slice the image vertically and create a composite x-z image using the maximum pixel values from all re-sliced x-z focal planes. A composite z line was then created using the maximum pixel from each column of the x-z composite plane, and a full width at half maximum (FWHM) measurement in the z-direction was made by fitting a polynomial spline. All pixel values were background subtracted using the mean pixel value from around the ball in the plane of best focus. The composite z-FWHM thus calculated (which depends on the size of the imaged ball) was used as a measure of the inter-plane resolution, or z-resolution.

2.5 Alignment

The alignment of the imaged volume to the compressed volume was assessed at the top and bottom of the volume. In order to assess vertical alignment, small high contrast markers (staples) were placed on the breast support table and on the underside of the compression paddle, and the image planes were inspected to check whether all markers were brought into focus within the reconstructed tomosynthesis volume. This was first done with no compression applied and then repeated with the chest wall edge of the paddle supported and 100N compression applied.

2.6 Image uniformity and repeatability

The reproducibility of the tomosynthesis exposures was tested by acquiring a series of 5 images of a 45mm thick block of PMMA using AEC. A 10mm x 10mm ROI was positioned 60mm from the chest wall edge in the plane corresponding to a height of 22.5mm above the breast support table. The mean and standard deviation of the pixel values in the ROI were found and the SNR was calculated for each image. These images and others acquired during the course of the evaluation were evaluated for artefacts by visual inspection.

The set of 16 tomosynthesis images of the CDMAM phantom was also used to test the repeatability of the reconstructed tomosynthesis images. The signal-to-noise ratio (SNR) was calculated in a uniform area within the CDMAM phantom in the same position in the in-focus plane from each reconstructed image.

2.7 Detector response

The detector response was measured for the detector operating in tomosynthesis mode. A 2mm thick aluminium filter was placed in the beam and attached to the tube port. The compression paddle was removed. The beam qualities 29kV W/Rh was selected and images were acquired using a range of tube load settings in tomosynthesis mode. The air kerma was measured and corrected using the inverse square law to give the air kerma incident at the detector. No corrections were made for the attenuation of X-rays by the breast support or anti-scatter grid. A 10mm x 10mm ROI was positioned on the midline, 50mm from the chest wall edge of the central projection image. The mean pixel value was measured and plotted against air kerma incident at the detector.

2.8 Timings

Using a stopwatch, image timings were measured whilst imaging a 45mm thickness of PMMA using AEC. Scan times were measured, from when the exposure button was pressed until the compression paddle was released, to when the reconstructed image appeared and to the moment when it was possible to start the next exposure.

2.9 Modulation transfer function

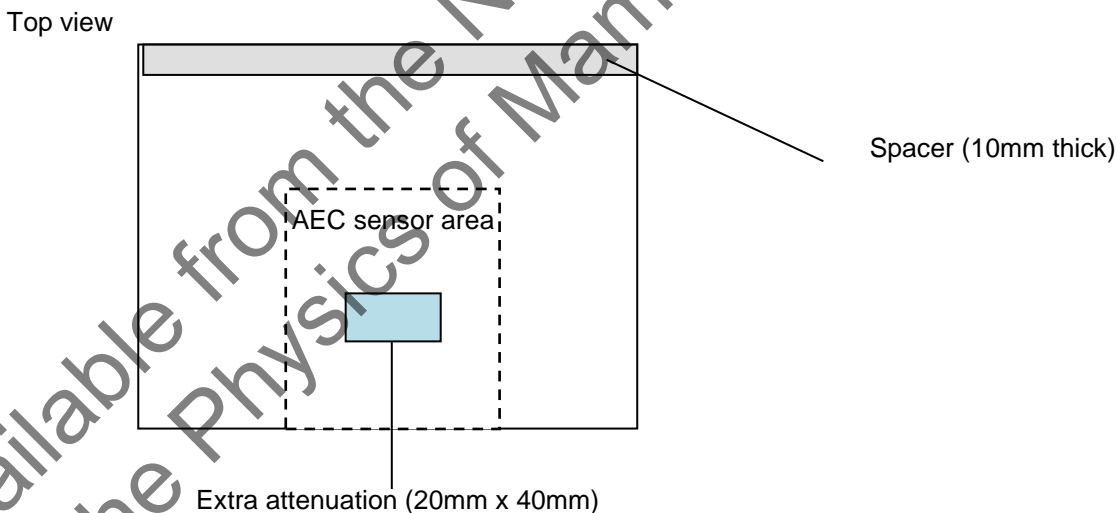
Modulation transfer function (MTF) measurements were made in tomosynthesis projection images as described in the EUREF protocol.⁷ The radiation quality used for the measurements was adjusted by placing a uniform 2mm thick aluminium filter at the tube housing. The beam quality used was 29kV W/Rh. The test device to measure the MTF comprised a 100mm x 80mm rectangle of stainless steel with a polished straight edge, of thickness 2mm. This test device was placed directly on the breast support table and at 40mm and 75mm above the breast support table. The test device was positioned to measure the MTF in 2 directions, first almost perpendicular to the CWE (direction of tube motion) and then almost parallel to it.

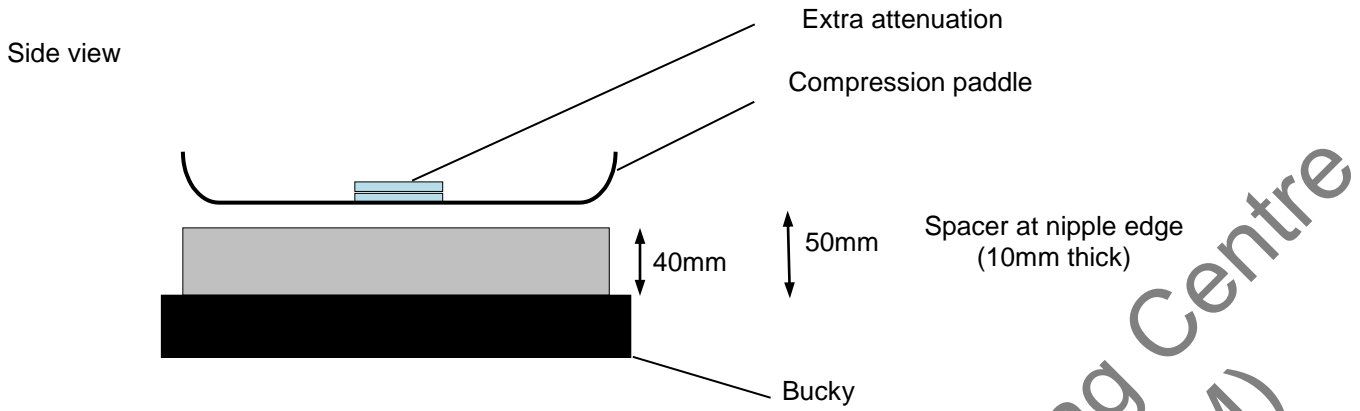
2.10 Local dense area

This test is described in the EUREF protocol.⁷ Images of a 40mm thick block of PMMA, of size 180mm x 240mm, were acquired using AEC. Extra pieces of PMMA between 2 and 20mm thick and of size 20mm x 40mm were added to provide extra attenuation. The compression plate remained in position at a height of 50mm, as shown in Figure 3. The simulated dense area was positioned 50mm from the CWE of the table.

In the simulated local dense area the mean pixel value and standard deviation for a 10mm x 10mm ROI were measured and the SNRs were calculated for the central projection images.

Figure 3. Setup to measure AEC performance for local dense areas





Available from the National Co-ordinating Centre
for the Physics of Mammography (NCCPM)

3. Results

3.1 Dose and contrast-to-noise ratio using AEC

The measurements of HVL and tube output of the system in tomosynthesis mode are summarised in Table 3.

Table 3. HVL and tube output measurement in tomosynthesis mode

kV	Target/filter	HVL (mm Al)	Output ($\mu\text{Gy/mAs}$ at 1m)
25	W/Rh	0.49	7.6
28	W/Rh	0.53	10.6
31	W/Rh	0.55	13.5
34	W/Rh	0.57	16.3

The MGDs to the standard breast model are shown in Figure 4. All MGDs include the preliminary exposure (5mAs), which is not used in the reconstruction of the tomosynthesis planes. The dose limiting value from the EUREF protocol⁷ is shown. The MGDs are shown in Table 4.

Figure 4. MGD for tomosynthesis exposures acquired using AEC for different equivalent breast thickness. Error bars indicate 95% confidence limits.

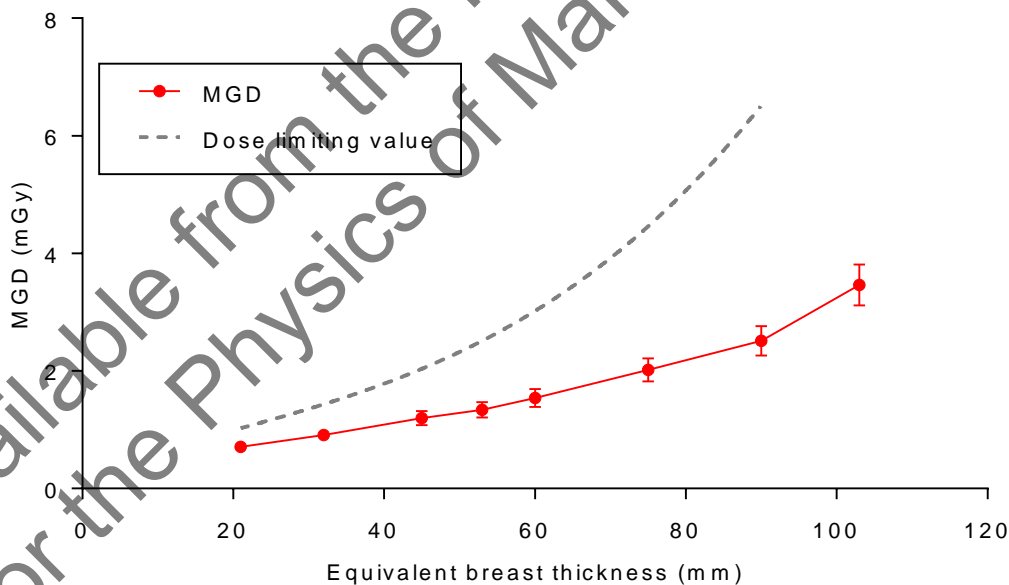


Table 5. MGD for tomosynthesis images acquired using AEC

PMMA thickness (mm)	Equivalent breast thickness (mm)	kV	Target/filter	mAs	MGD (mGy)	Dose limiting value (mGy)	Displayed dose (mGy)	Displayed % higher than MGD
20	21	26	W/Rh	59.5	0.71	1.2	0.89	25.5
30	32	27	W/Rh	85.5	0.91	1.5	1.15	26.8
40	45	28	W/Rh	123.8	1.20	2.0	1.44	19.7
45	53	29	W/Rh	138.0	1.34	2.5	1.55	15.9
50	60	30	W/Rh	153.3	1.54	3.0	1.70	10.7
60	75	31	W/Rh	210.3	2.02	4.5	2.10	3.9
70	90	32	W/Rh	275.6	2.51	6.5	2.66	5.9
80	103	32	W/Rh	427.0	3.46	-	3.70	6.9

Figure 5 shows the CNRs measured in focal planes and central projection images. The CNRs are shown in Table 6. Figure 6 shows the CNR in the projection images at different projection angles.

Figure 5. CNR for tomosynthesis images acquired using AEC for different equivalent breast thickness. Error bars indicate 95% confidence limits.

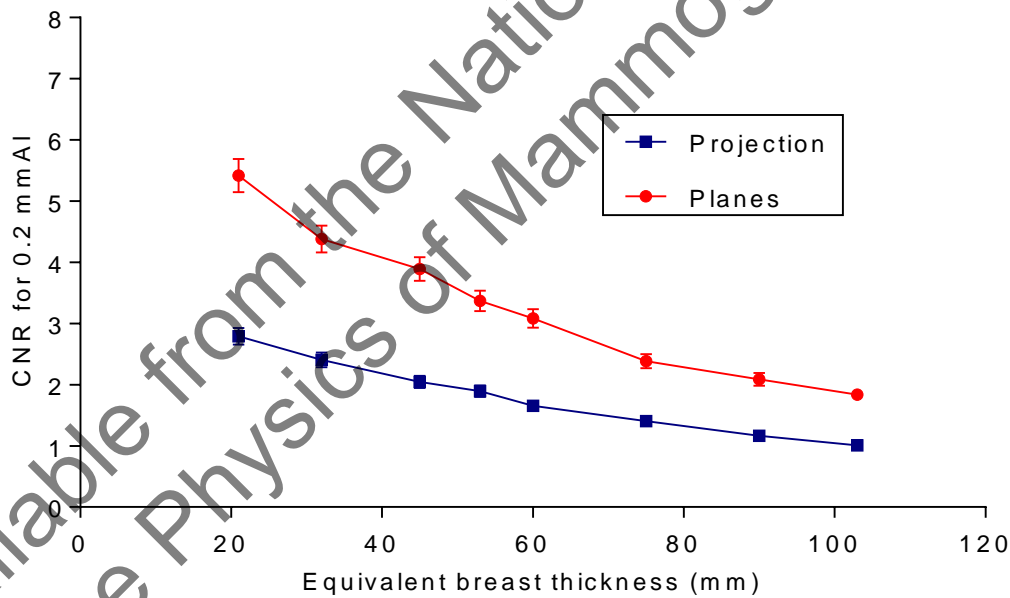
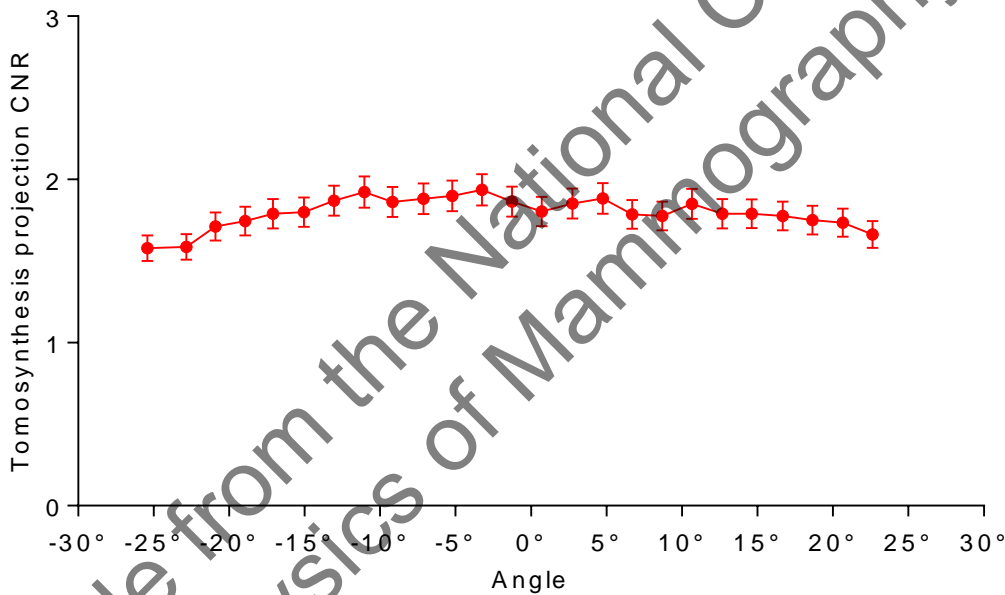


Table 6. CNR for tomosynthesis images acquired using AEC

PMMA thickness (mm)	Equivalent breast thickness (mm)	kV	Target/filter	mAs	CNR	
					Focal planes	Central projections
20	21	26	W/Rh	59.5	5.41	2.79
30	32	27	W/Rh	85.5	4.38	2.40
40	45	28	W/Rh	123.8	3.89	2.04
45	53	29	W/Rh	138.0	3.37	1.90
50	60	30	W/Rh	153.3	3.08	1.65
60	75	31	W/Rh	210.3	2.39	1.40
70	90	32	W/Rh	275.6	2.09	1.17
80	103	32	W/Rh	427.0	1.84	1.01

Figure 6. Variation of projection CNR with angle for images of 45mm PMMA. Error bars indicate 95% confidence limits.



3.2 Image quality measurements

The lowest threshold gold thicknesses were obtained for focal plane 26. In Figure 7 the threshold gold thicknesses are shown for focal plane 26 at approximately the AEC dose and twice and half the AEC dose. The threshold gold thicknesses shown in Figure 7 are summarised in Table 7.

Figure 7. Threshold gold thickness for plane 26, at 3 dose levels. Error bars indicate 95% confidence limits.

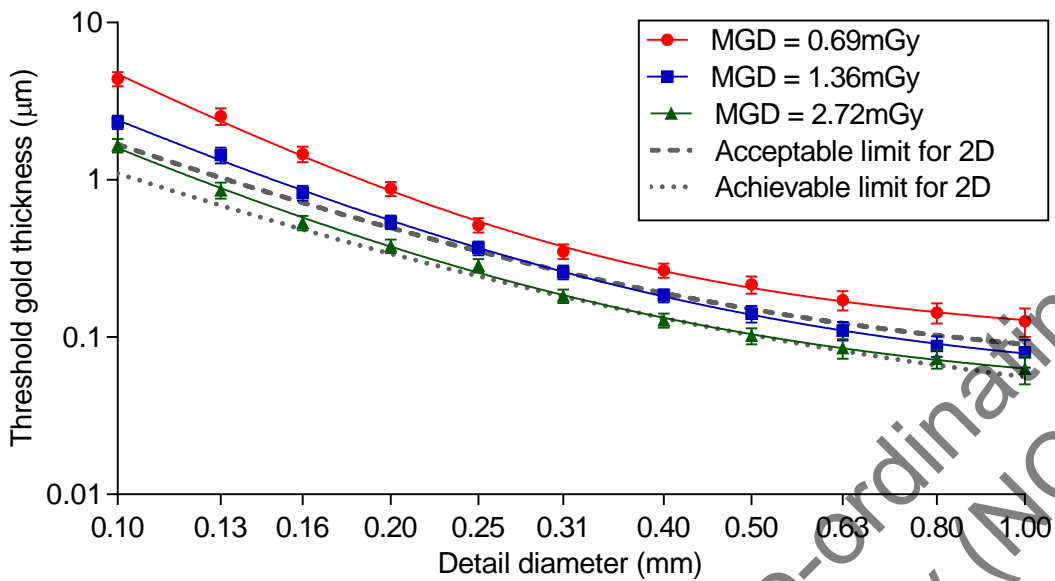


Table 7. Threshold gold thickness for reconstructed focal plane 26 of the image of the CDMAM phantom (automatically predicted data)

Detail diameter (mm)	Threshold gold thickness (µm)		
	Plane (0.69mGy)	Plane (1.36mGy)	Plane (2.72mGy)
0.1	4.39 ± 0.44	2.33 ± 0.23	1.66 ± 0.16
0.25	0.52 ± 0.05	0.37 ± 0.04	0.29 ± 0.03
0.5	0.22 ± 0.03	0.14 ± 0.02	0.10 ± 0.01
1.0	0.13 ± 0.03	0.08 ± 0.02	0.063 ± 0.013

3.3 Geometric distortion and resolution between focal planes

3.3.1 Height of best focus

All balls within each image were brought into focus at the same height (± 1 mm) above the table, and within 1mm of the expected height. The phantom was tilted to be parallel to the detector. This indicates that the focal planes are flat and parallel to the detector but not to the breast support table. There was no noticeable vertical distortion found in the image stack.

Additional planes are reconstructed below the breast support table and the first focal plane corresponds to approximately 1mm below the breast support table. The number of focal planes reconstructed is equal to the indicated breast thickness in millimetres plus 1.

3.3.2 Positional accuracy within focal plane

No significant distortion or scaling error was seen within focal planes. Scaling errors, in both the x and y directions, were found to be less than 0.5%. Maximum deviation from the average distance between the balls was 0.28mm in the x and y directions, compared to the manufacturing tolerance of 0.1mm in the positioning of the balls.

3.3.3 Appearance of the ball in adjacent focal planes

In the plane of best focus the aluminium balls appeared well-defined and circular. When viewing successive planes, moving away from the plane of best focus, the images of the balls shrank in the direction parallel to the CWE. The changing appearance of one of the balls through successive focal planes is shown in Figure 9.

Figure 9. Appearance of 1mm aluminium balls in reconstructed focal planes at 1mm intervals, from 4mm below to 3mm above the plane of best focus.

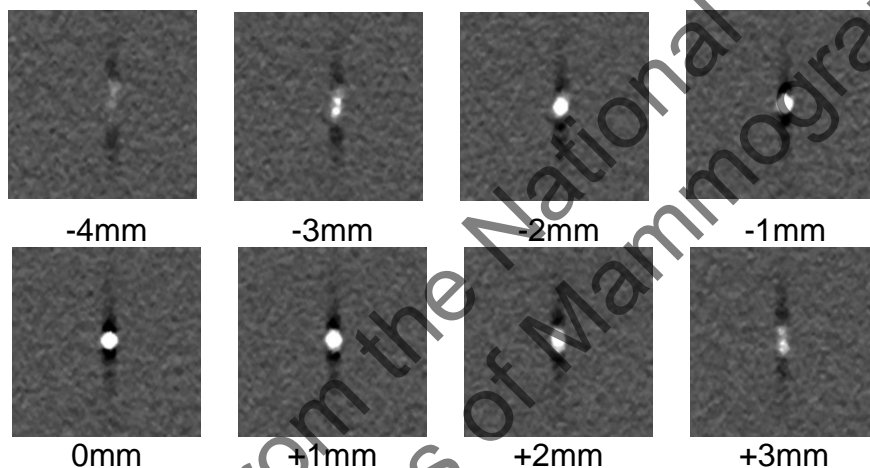
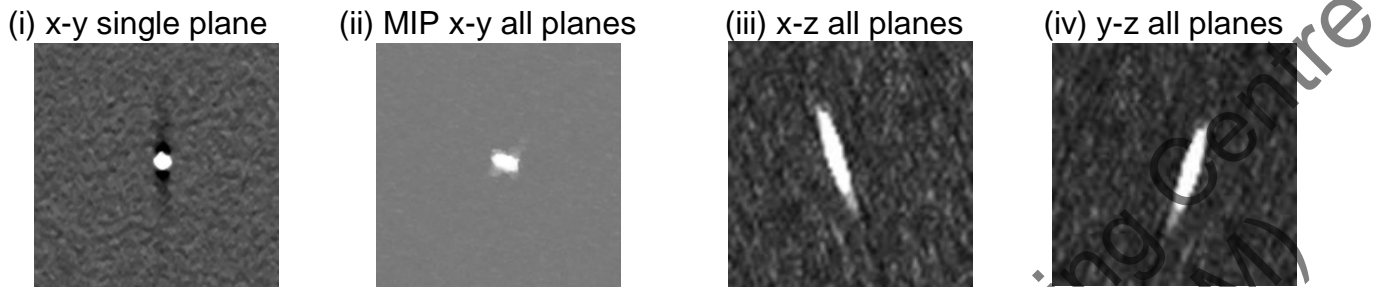


Image extracts for a ball positioned in the central area, 120mm from the chest wall, are shown in Figure 10. In these images, pixels within the focal plane represent dimensions of approximately 0.1mm x 0.1mm. The spacing of reconstructed focal planes is 1mm.

Figure 10. Extracts from planes showing 1mm aluminium ball in (i) single focal plane, (ii) Maximum Image Projection (MIP) through all focal planes, and through re-sliced vertical planes in the directions (iii) parallel and (iv) perpendicular to the chest wall.



Measurements of the z-FWHM of the reconstruction artefact associated with each ball are summarised in Table 8 for images of balls at heights of 7.5mm, 32.5mm and 52.5mm above the breast support table.

Table 8. z-FWHM measurements of 1mm diameter aluminium balls

z-FWHM (range)	
Planes	6.8mm (6.4 to 7.0)

3.4 Alignment

The alignment of the X-ray field to the focal plane at the surface of the breast support table was assessed. At the CWE the X-ray field overlapped the reconstructed tomosynthesis image by 0mm.

The staples on the breast support and under the paddle were brought into focus within the reconstructed volume. The staples positioned on the breast support were not all brought into focus in a single plane due to the tilt of the breast support. Staples positioned towards the CWE were brought into focus in the 2nd plane whilst staples positioned approx. 19cm back from the CWE were brought into focus in plane 4. With 100N compression applied and only the CWE of the paddle supported, the staples under the compression paddle near the CWE of the paddle were in focus within the reconstructed volume.

There was no missed tissue at the bottom or top of the reconstructed volume.

3.5 Image uniformity and repeatability

In tomosynthesis mode the AEC selected the same tube voltage and target/filter combination for each of the 5 repeat exposures, and the tube load varied by a maximum of 0.2%. For exposures repeated during the 4 days of the evaluation the tube load varied by a maximum of 0.5%, within the 5% limiting value in the EUREF protocol.⁶

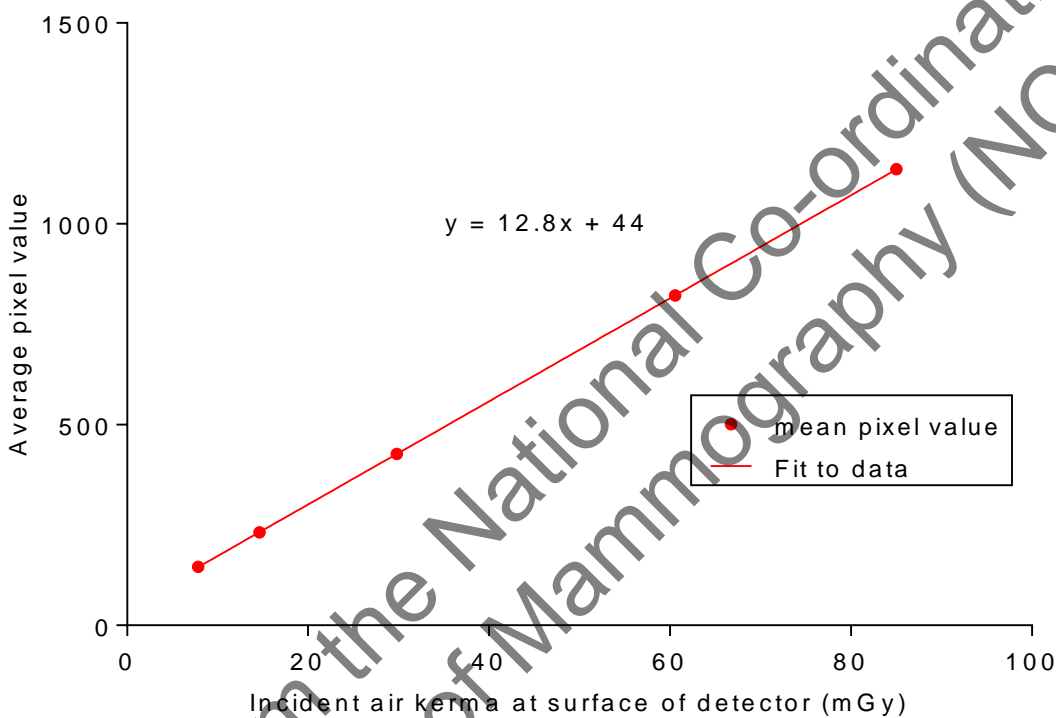
In the test of repeatability of the tomosynthesis reconstruction, using images of the CDMAM phantom, the maximum deviation from the mean SNR was found to be 4.7%.

The reconstructed images of plain PMMA were uniform with no visible artefacts.

3.6 Detector response

The detector response for the central projection of tomosynthesis images acquired at 29kV W/Rh is shown in Figure 12.

Figure 12. Detector response in tomosynthesis mode



3.7 Timings

Scan times for tomosynthesis only and tomosynthesis plus 2D combination modes are shown in Table 9. The times between consecutive exposures and between initiating the exposure to the release of the compression paddle were measured for acquiring images for a 53mm compressed breast thickness. These times include time for the reconstruction of the tomosynthesis planes and so those values will be related to the thickness of the volume being reconstructed.

Table 9. Scan and reconstruction timings

	Time
Tomosynthesis only	
Time from start of exposure until decompression	29s
Time from start of exposure until next exposure is possible	80s
Time from decompression until reconstructed image displayed	80s
Combination mode (Tomosynthesis plus 2D)	
Time from start of exposure until decompression	41s
Time from start of exposure until next exposure is possible	88s

3.8 Modulation Transfer Function

MTF results for the central projection images are shown in Figure 13. Results are shown in the 2 orthogonal directions parallel (u) and perpendicular (v) to the tube axis, at 0mm, 40mm and 75mm above the surface of the breast support table. The x-ray tube moves in the v direction. These results are summarised in Table 10.

Figure 13. MTF for tomosynthesis central projections

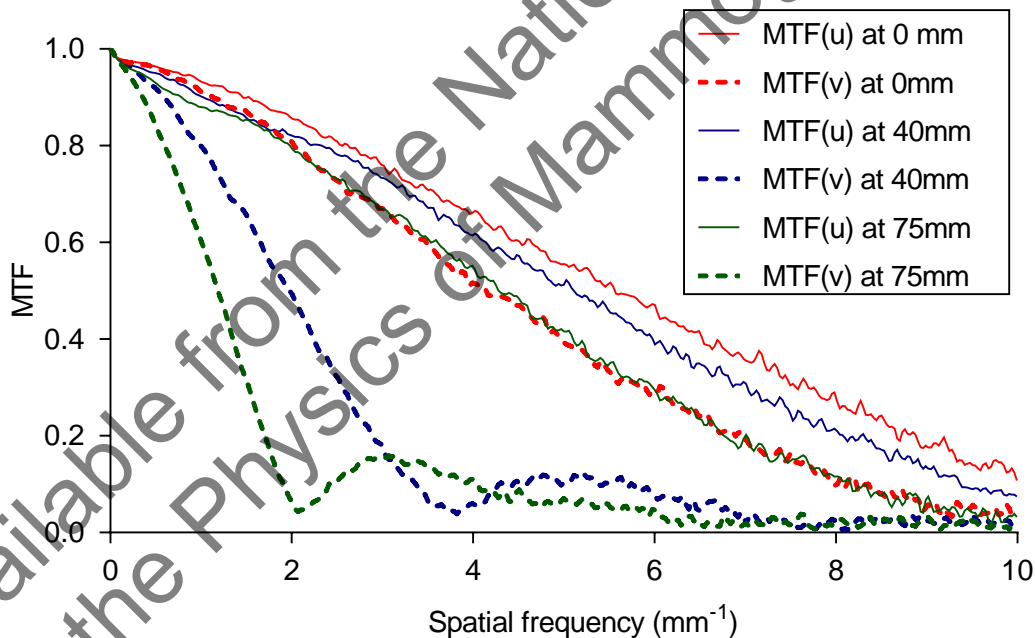


Table 10. MTF for central projections in the directions parallel (u) and perpendicular (v) to the tube axis

Spatial frequency (mm ⁻¹)	0mm above table		40mm above table		75mm above table	
	u	v	u	v	u	v
0	1.00	1.00	1.00	1.00	1.00	1.00
1	0.91	0.91	0.90	0.81	0.89	0.56
2	0.86	0.81	0.82	0.48	0.79	0.15
3	0.78	0.67	0.73	0.17	0.67	0.11
4	0.67	0.52	0.62	0.07	0.54	0.12
5	0.55	0.38	0.51	0.10	0.41	0.07
6	0.44	0.27	0.40	0.09	0.29	0.02
7	0.34	0.19	0.30	0.04	0.19	0.02
8	0.25	0.13	0.21	0.01	0.11	0.03
9	0.18	0.08	0.13	0.03	0.06	0.02
10	0.13	0.05	0.07	0.02	0.03	0.02

The spatial frequencies of the 50% MTF (MTF₅₀) are shown in Table 11.

Table 11. MTF₅₀ for central projection

	u-direction	v-direction
0mm	5.45mm ⁻¹	4.14mm ⁻¹
40mm	5.07mm ⁻¹	1.94mm ⁻¹
75mm	4.32mm ⁻¹	1.10mm ⁻¹

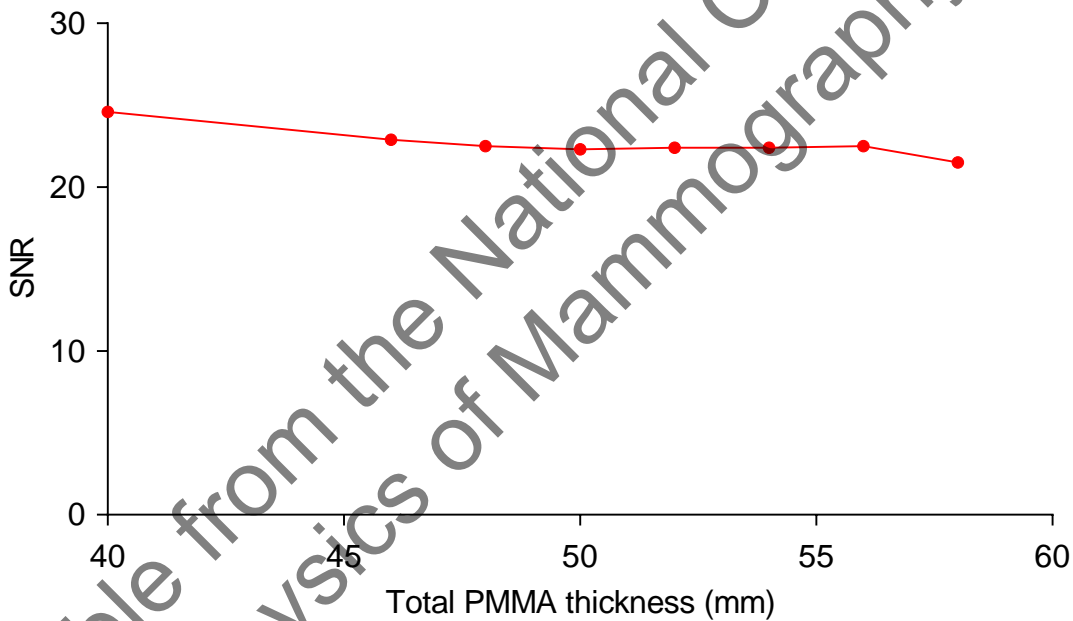
3.9 Local dense area

The test in the EUREF protocol⁷ is based on an assumption that when the AEC adjusts for local dense areas, the SNR should remain constant with increasing thickness of extra PMMA. The results are presented in Table 12 and Figure 14. The results show that the mAs was increased with the addition of the small pieces of PMMA, indicating that the AEC adjusts for local dense areas in tomosynthesis mode. The results show a small decrease in SNR between 40mm and 58mm of PMMA but results are well within the 20% tolerance.⁷ There was no change in the kV and anode/filter combination selected.

Table 12. AEC performance for local dense areas, measured on the midline and 50mm from the CWE

Total attenuation (mm PMMA)	kV	Target/ filter	Tube load (mAs)	SNR	% SNR difference from mean SNR
40	29	W/Rh	126	24.6	8.1
46	29	W/Rh	132	22.9	0.4
48	29	W/Rh	140	22.5	-1.3
50	29	W/Rh	149	22.3	-2.1
52	29	W/Rh	158	22.4	-1.5
54	29	W/Rh	171	22.4	-1.7
56	29	W/Rh	182	22.5	-1.1
58	29	W/Rh	179	21.5	-5.5

Figure 14. AEC performance in projection images for local dense areas



4. Discussion

4.1 Dose and contrast-to-noise ratio

The MGDs in tomosynthesis mode were lower than the dose limiting values set for tomosynthesis systems in the EUREF protocol.⁷

CNRs in projections and the resultant reconstructed planes showed a steady decrease with increasing breast thickness.

4.2 Image quality

In the absence of any better test object for assessing tomosynthesis imaging performance, images of the CDMAM test object were acquired in tomosynthesis modes. At the dose close to that selected by the AEC, the threshold gold thickness for reconstructed focal planes was better than the minimum acceptable level that is applied to 2D mammography for disk diameters greater than 0.25mm. Results were determined for focal plane number 26, which gave the best results. For double and half the AEC selected dose, the threshold gold thickness changed as expected.

These results take no account of the ability of tomosynthesis to remove the obscuring effects of overlying tissue in a clinical image, and the degree of this effect is expected to vary between tomosynthesis systems. There is as yet no standard test object that would allow a realistic and quantitative comparison of tomosynthesis image quality between systems or between 2D and tomosynthesis modes. A suitable test object would need to incorporate simulated breast tissue to show the benefit of removing overlying breast structure in tomosynthesis imaging, as compared to 2D imaging.

4.3 Geometric distortion and reconstruction artefacts

Assessment of geometric distortion demonstrated that the reconstructed tomosynthesis focal planes were flat and parallel to the detector rather than to the breast support, which is tilted. No vertical or in-plane distortion was seen and there were no significant scaling errors.

The reconstructed tomosynthesis volume starts about 1mm below the surface of the breast support table and continues 1mm above the nominal height of the compression paddle. This is useful in that it allows for a small margin of error in the calibration of the indicated thickness or some slight tilt of the compression paddle, without missing tissue at the bottom or top of the reconstructed image.

The mean inter-plane resolution (z-FWHM) for the 1mm diameter balls was 6.8mm.

There is a maximum of 100 planes. If the breast or test object is thicker than 100mm then a warning is given that any part of the object above this height will not be reconstructed.

4.4 Alignment

The alignment of the X-ray beam to the reconstructed image was satisfactory. There was no missed tissue at the bottom or top of reconstructed tomosynthesis images.

4.5 Image uniformity and repeatability

The repeatability of tomosynthesis AEC exposures and the repeatability of tomosynthesis reconstructions were satisfactory with values of 0.5 and 4.7% respectively, below the limit of 5%.

4.6 Modulation transfer function

Large differences are seen in the MTFs between the 2 orthogonal directions, especially at 40mm and 75mm above the breast support. The system acquires images while the x-ray tube is moving and this causes the v-direction (direction of tube motion) in the image to have a lower MTF.

4.7 Local dense area

The EUREF protocol⁷ states that the system is expected to adjust the exposures in response to the thickness of added small pieces of PMMA. A provisional tolerance was that the SNR is kept within 20% of the average SNR.

The Siemens Revelation undertakes a low dose pre-exposure to set the radiographic factors. The factors are adjusted according to the densest area detected in the image. The results show that the system increases the tube loading up to an added thickness of 18mm. For increasing thicknesses of PMMA a small decrease in the SNR was seen but this was within the 20% tolerance.

5. Conclusions

The technical performance of the Siemens Revelation digital breast tomosynthesis system was found to be satisfactory. At the moment, no image quality standards have been established for digital breast tomosynthesis systems.

The MGD to the 53mm thick standard breast in tomosynthesis mode was found to be 1.34mGy. This is below the dose limiting value of 2.5mGy for tomosynthesis.⁷

Available from the National Co-ordinating Centre
for the Physics of Mammography (NCCPM)

References

1. Studley CJ, Looney P, Young KC. Technical evaluation of Hologic Selenia Dimensions digital breast tomosynthesis system (NHSBSP Equipment Report 1307 Version 2). Sheffield: NHS Cancer Screening Programmes, 2014
2. Strudley CJ, Warren LM, Young KC. Technical evaluation of Siemens Mammomat Inspiration digital breast tomosynthesis system (NHSBSP Equipment Report 1306 Version 2). Sheffield: NHS Cancer Screening Programmes, 2015
3. Strudley CJ, Oduko JM, Young KC. Technical evaluation of GE Healthcare SenoClaire digital breast tomosynthesis system (NHSBSP Equipment Report 1404). London: Public Health England, 2016
4. Strudley CJ, Hadjipanteli A, Oduko JM, Young KC. Technical evaluation of Fujifilm AMULET Innovality digital breast tomosynthesis system (NHSBSP Equipment Report). London: Public Health England, 2018
5. Strudley CJ, Oduko JM, Young KC. Technical evaluation of IMS Giotto Class digital breast tomosynthesis system (NHSBSP Equipment Report). London: Public Health England, 2018
6. Burch A, Loader R, Rowberry B et al. Routine quality control tests for breast tomosynthesis (physicists) (NHSBSP Equipment Report 1407). London: Public Health England, 2015
7. van Engen RE, Bosmans H, Bouwman RW et al. Protocol for the Quality Control of the Physical and Technical Aspects of Digital Breast Tomosynthesis Systems. Version 1.03. www.euref.org 2018
8. Dance DR, Young KC, van Engen RE. Estimation of mean glandular dose for breast tomosynthesis: factors for use with the UK, European and IAEA breast dosimetry protocols. *Phys. Med. Biol.*, 2011, 56, 453-471.
9. Marshall N W and Bosmans H. Measurements of system sharpness for two digital breast tomosynthesis systems. *Phys. Med. Biol.*, 2012, 57, 7629–50